Optimization of Computer-Generated Transmission Holograms Using Different LED Wavefront Approximations

Daniela Karthaus*, Markus Giehl*, Oliver Sandfuchs**, Stefan Sinzinger***

*L-LAB - research institute for automotive lighting and mechatronics, Lippstadt, Germany
**University of Applied Sciences Hamm-Lippstadt, Germany
***Ilmenau University of Technology, Germany

mailto:daniela.karthaus@l-lab.de

The reconstruction of computer-generated transmission volume holograms with light-emitting diodes (LEDs) requires the adaptation of the holograms to the specific diodes' wavefronts. We show first results of the analysis of different LED wavefront approximations, including a new interferometry-based approach to measure an LED wavefront.

1 Introduction

The application of computer-generated transmission holograms in automotive headlamps is accompanied by the reconstruction of the holograms with typical automotive light sources. A well-established light source is the phosphor-converted LED, which shows large divergence angles up to ±60°. To avoid scaling and blurring effects of the reconstructed image (c.f. Ref. [1,2]), the holograms must be optimized for the specific wavefront of a LED. While various wave properties of LEDs are regarded in literature (c.f. Ref. [3-5]), the specific wavefront shape of LEDs is not addressed or only approximated by ideal wavefront descriptions [6,7]. To identify the most appropriate wavefront approximation for a LED, different approaches are used within the hologram design. It is assumed, that the best approximation of the LED leads to a minimum deviation between the appearance of the reconstructed image and the desired image. As a criterion for the similarity between the ideal image and the reconstructed image the correlation coefficient ρ is used. A higher coefficient value indicates a higher similarity and a better LED approximation. In this paper an automotive-certified white LED (Luxeon F, Philips) is used.

2 LED wavefront descriptions

One option to approximate an LED's wavefront is the description as a spherical wave (SW) (c.f. Ref. [7]). In fact, the dimension of the LED's light-emitting surface is not ideally small. It is expected, that the consideration of the real dimensions would lead to a more realistic approximation. Therefore, the Huygens' principle (HP) can be used [8]. In this case, the LED's wavefront is approximated by the envelope of M x N ideal spherical waves that are located on the LED's surface. The Rayleigh-Sommerfeld (RS) approximation is another way to describe this principle. In this paper, the convolution-based RS approximation is used (c.f. Ref. [9,10]). From a theoretical point of view, these descriptions are appropriate ways to approximate the LED's wavefront. However, the specific emission characteristic of the LED resulting from additional lenses or converting materials is not considered in these approaches. For this reason, a new approach is used to measure the specific wavefront [11].

The approach is based on a Mach-Zehnder interferometer to interfere a spherical reference wave and the desired sample wave. The interference pattern is recorded with a CCD detector and the LED's phase information are calculated with a two-step phase-shifting algorithm [11]. The results are denoted as measured wave (MW) in this paper. To get analyzable interference images, the light of the LED is filtered with a polarizer and a narrowband bandpass filter. Different filters at peak wavelengths of λ_g=532 nm, λ_a=590 nm and λ_r=620 nm, each with a bandwidth of $\Delta\lambda$=10 nm, are used.

3 Hologram optimization

Four holograms are designed, each for one of the four different LED wavefront approximations presented in section 2. The reconstructed image of each hologram is supposed to show a defined test pattern, which is projected on a screen at a distance of 300mm behind the holograms. Therefore, the holograms are designed within a three-step process as a matrix that is composed of L x K subholograms [11]. Within the first step, the holographic information of the basic hologram is calculated with the Gerchberg-Saxton algorithm [12]. In the second step, the basis-hologram is replicated and the local phase information of a lens is added to each of the L x K subholograms to overlap all reconstructed images at the same local position on the screen. At this point, the test pattern would be reconstructed correctly, if the hologram is illuminated with a plane wave. To adapt the hologram to the reconstruction wave of the LED, the complex conjugate of the local phase pattern is calculated using one of the LED approximations as discussed in section 2 and is

submitted: 20.Jul.2017 published: 07.Aug.2017

added to the phase information of each subhologram at the same image position. The four designed holograms are exposed into a photopolymer and illuminated with the filtered LED. The reconstructed images are recorded with a camera and the correlation coefficient is calculated for each approximation. The highest value for ρ, that was achieved within a pretest, is ρ=0.863±0.007 for an ideally reconstructed hologram with laser illumination.

4 Results

The reconstructed images and, consequently, the values of the correlation coefficient differ depending on the considered LED approximation. In Fig. 1 the values are illustrated for the results at 532nm.

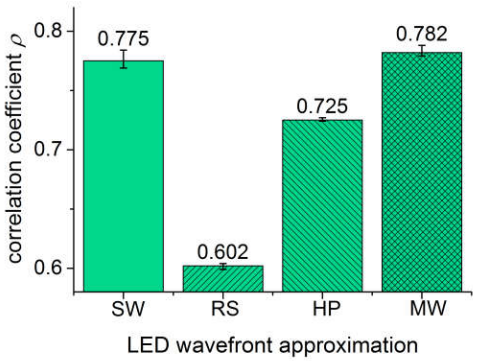

Fig. 1: Calculated correlation coefficient compared between the reconstructed and the ideal image for the different wavefront approximations.

Obviously, the RS and the HP approximations lead to lower values (ρ_{RS}=0.602±0.003, ρ_H=0.725±0.002) than the SW and the MW approximation (ρ_S=0.775±0.007, ρ_M=0.782±0.005). The MW leads to the highest value and shows only a slight deviation of $|\Delta\rho|$=0.007 from the value of the SW. In contrast, the differences between the SW and the RS and the SW and the HP approximation are clearly higher ($|\Delta\rho|$=0.173 for RS and $|\Delta\rho|$=0.05 for HP). The same tendencies are found for additional experiments at 532nm, 590nm and 620nm [11].

5 Discussion and Outlook

Using the value of ρ as an indicator for the quality of the LED approximations, the RS and the HP approximations are not appropriate, although they were assumed to describe the LED's wave in the most realistic way. This might be caused by the negligible influence of the light converting phosphor, which is used to realize the white light emission of the LED. The phosphor leads to a diffuse Lambertian emission. Assuming the validity of the theory of the normal congruence of rays and waves for the LED, the presented results are more reasonable. A Lambertian characteristics shows a stronger curvature than all approximations considered here, and the curvatures of the MW and the SW are closer to a Lambertian characteristics than the RS and the HP approximation. However, this assumption must be regarded in further test series. One additional important aspect is the angular region, for which the approximations are compared. Due to limitations of the interferometric setup, the measurable region covers only ±2°, while the LED emits into a region of ±60°. It is assumed that the difference between a SW and the actually emitted wave becomes stronger for larger angles. Thus, the interferometric setup has to be improved and relations between the wave-optical and the ray-optical measurements of the LED emission have to be investigated.

References

[1] E. G. Loewen, E. Popov, *Diffraction gratings and applications*, (Marcel Dekker Inc. 1997)

[2] D. Karthaus, O. Sandfuchs, S. Sinzinger, “Optimization of holograms for application in automotive headlamps with LED illumination,” in *Applied Industrial Optics: Spectroscopy, Imaging and Metrology, OSA technical digest* (online), p. JW4A.17 (2016)

[3] I. Moreno, C.-C. Sun, “Modeling the radiation pattern of LEDs,” *Opt. Express* **16**(3), 1808–1819 (2008)

[4] J. Tervo, J. Turunen, P. Vahimaa, F. Wyrowski, “Shifted-elementary-mode representation for partially coherent vectorial fields,” *JOSA A* **27**(9), 2004–2014 (2010)

[5] P. Petruck, R. Riesenberg, R. Kowarschik, “Partially coherent light-emitting diode illumination for video-rate in-line holographic microscopy,” *Appl. Opt*. **51**(13), 2333–2340 (2012)

[6] F. Wyrowski, H. Schimmel, M. Kuhn, “Elektromagnetisches Optikrechnen – Modellierung realer Lichtquellen,” *Photonik* **39**(2), 66–70 (2007)

[7] T. Kari, J. Gadegaard, T. Sondergaard, T. G. Pedersen, K. Pedersen, “Reliability of point source approximations in compact LED lens designs,” *Opt. Express* **19**(6), A1190–A1195 (2011)

[8] M. Born, E. Wolf, A. B. Bhatia, *Principles of optics: Electromagnetic theory of propagation, interference and diffraction of light*, (Cambridge Univ. Press 2016)

[9] K. Matsushima, T. Shimobaba, “Band-limited angular spectrum method for numerical simulation of free-space propagation in far and near fields,” *Opt. Express* **17**(22), 19,662–19,673 (2009)

[10] F. Shen, A. Wang, “Fast-Fourier-transform based numerical integration method for the Rayleigh-Sommerfeld diffraction formula,” *Appl. Opt.* **45**(6), 1102–1110 (2006)

[11] D. Karthaus, M. Giehl, O. Sandfuchs, S. Sinzinger, “Modeling of light-emitting diode wavefronts for the optimization of transmission holograms,” *Appl. Opt.* **56**(18), 5234–5241 (2017)

[12] R. W. Gerchberg, W. O. Saxton, “A practical algorithm for the determination of the phase from image and diffraction plane pictures,” *Optik* **35**, 237-246 (1972).

submitted: 20.Jul.2017 published: 07.Aug.2017